J Solid State Electrochem (2012) 16:2675–2681
DOI 10.1007/s10008-012-1674-y

ORIGINAL PAPER

Direct electrochemical non-enzymatic assay of glucose using functionalized graphene

Malledevaru Mallesha · Revanasiddappa Manjunatha · Gurukar Shivappa Suresh · Jose Savio Melo · S. F. D'Souza · Thimmappa Venkatarangaiah Venkatesha

Received: 14 October 2011 / Revised: 19 January 2012 / Accepted: 30 January 2012 / Published online: 28 February 2012

Abstract A non-enzymatic amperometric sensor is developed based on the graphite electrode modified with functionalized graphene for the determination of β, D (+)-glucose. Cyclic voltammetry and electrochemical impedance spectroscopy techniques are used to study the behavior. Atomic force microscopy was used to study the surface topography of the working electrode before and after its modification. The sensor enabled the direct electrochemical oxidation of β, D (+)-glucose in alkaline medium and responded linearly to the analyte over the range from 0.5×10^{-3} to 7.5×10^{-3} M with a limit of detection of 10 μM. The sensor is found to exhibit a better sensitivity of 28.4 μA mM^{-1} cm^{-2}, good stability, and shelf life. The sensitivity of the sensor to β, D (+)-glucose was not affected by the commonly co-existing interfering substances such as L-ascorbic acid, dopamine, uric acid, and acetaminophen.

Keywords Non-enzymatic · β, D (+)-glucose · Functionalized graphene · Sensor · Modification

M. Mallesha · R. Manjunatha · G. S. Suresh (✉)
Chemistry Research Centre, S.S.M.R.V. Degree College, Jayanagar,
Bangalore 560041, India
e-mail: sureshssmrv@yahoo.co.in

J. S. Melo · S. F. D'Souza
Nuclear Agriculture and Biotechnology Division,
Bhabha Atomic Research Centre,
Mumbai 400085, India

T. V. Venkatesha
Department of Chemistry, Kuvempu University,
Jnana Sahyadri,
Shimoga 577451, India

Introduction

A number of industrial, biotechnological, and especially biomedical applications demand a simple, reliable, accurate, and rapid technique for the analysis of sugars, particularly glucose. It was estimated that in 2000, 2.8% of the world population was affected by *diabetes mellitus*, a disease with hyperglycemia (i.e., elevated blood glucose level) as the major symptom. So, determination of blood glucose remains a growing concern even though the clinical conditions of the disease are very clear and well understood. Ever since Clark [1] proposed the initial concept of an enzyme-based biosensor for glucose way back in 1962, a lot of research has been done to develop and fabricate a biosensor for glucose. Originally and until recently, in most of the glucose biosensors, glucose oxidase is used as the model enzyme which catalyzes the oxidation of β, D (+)-glucose into glucono-δ-lactone in the presence of molecular oxygen, simultaneously producing hydrogen peroxide. Then glucose is generally quantified by electrochemical oxidation of the liberated hydrogen peroxide or less commonly by the electrochemical reduction of the consumed oxygen. However, the former reaction occurs at a high positive potential (more than 0.6 V), and at this potential, many endogenous electroactive substances such as L-ascorbic acid (AA), uric acid (UA), and dopamine (DA), co-existing in biological fluids, are also oxidized, thus severely affecting the selectivity of the biosensor. Also, the greatest drawback of biosensors is their instability originating from the intrinsic nature of the enzyme. These limitations of the enzyme-based biosensors and the growing need for a stable, simple, reliable, and cost-effective sensor for glucose, particularly in the biomedical

field, have lead to the emergence of a new generation (also called the fourth generation) of amperometric glucose sensors, known as "non-enzymatic" or "enzyme-free" glucose sensors, that is, not involving any enzyme.

The pioneering work in the field of non-enzymatic glucose sensor was done in 1909 by Walther Loeb who electrocatalytically oxidized glucose in H_2SO_4 at a lead anode. In spite of decades of research in this field, the practical application of non-enzymatic glucose sensors was prevented mainly because of the lack of selectivity, sluggish kinetics of glucose oxidation at many of the bare electrodes, and fouling of electrode surface by the constituents of real samples such as chloride ions and proteins. However, with the advent of nano materials, there was a sudden surge in non-enzymatic systems. Various nanomaterials such as mesoporous platinum [2], nanoporous gold [3], platinum nanotube arrays [4], CuO nanowire arrays [5], alloys such as platinum–iridium alloy[6], platinum–lead nanoparticles [7], platinum–lead nano arrays [8], boron-doped diamond [9], carbon nanotubes [10], palladium nanoparticle–graphene nanocomposite [11], and so forth, have been used in the fabrication of non-enzymatic glucose sensors in order to alleviate some of their drawbacks as mentioned above. Majority of the non-enzymatic sensors rely on the current response of glucose oxidation directly at the electrode surface, the mechanism of which considerably depends on the electrode material used. Two models, namely activated chemisorptions model [12] and incipient hydrous oxide ad atom mediator model [13] have been proposed to explain the mechanism of electro-oxidation of glucose at various electrode materials.

Graphene is described as "the rising star carbon material" in the literature for it is the latest nano form of carbon to be discovered and is the current hottest topic in the field of material science. Structurally, it is a one-atom-thick two-dimensional sheet of bonded sp^2 carbon atoms that are densely packed in a honey-comb crystal lattice. It is an intriguing carbon material with extraordinary electrochemical, electronic, and mechanical properties comparable to or even better than those of carbon nanotubes [14]. The high surface area is helpful in increasing the surface loading of enzymes and other modifying molecules, while the excellent conductivity and small band gap are favorable for electronic conduction. Being such a unique material, graphene finds applications in various areas such as opto-electronic devices [15], super capacitors [16], gas sensors [17], pH sensors [18], and chemical sensors [19]. In the last few years, nanocomposites of graphene with polymers, metals, and metal oxides have been widely used in the fabrication of sensors for various biomolecules like dopamine [20], nicotinamide adenine dinucleotide [21], and glucose [22]. Therefore, graphene seems to be another promising material for developing of non-enzymatic glucose sensor.

In the present work, we have used functionalized graphene for developing an amperometric non-enzymatic glucose sensor. This sensor was found to exhibit better analytical parameters.

Experimental procedures

Reagents and instrumentation

D (+)-glucose, L-ascorbic acid, dopamine, uric acid, sodium hydroxide, and graphite electrodes (6 mm in diameter) were purchased from the Sigma-Aldrich company, USA. Reduced graphene sheets were purchased from Quantum Materials Corporation (India). All other chemicals used in this work are of analytical grade and were used as received. All aqueous solutions were prepared with high-quality doubly distilled water.

Cyclic voltammetry, chronoamperometry, and electrochemical impedance studies were performed using a VersaSTAT 3 from Princeton Applied Research (USA). All electrochemical experiments were carried out using a conventional single-compartment three-electrode system consisting of either a bare graphite electrode or graphite electrode modified with functionalized graphene as the working electrode, a platinum wire as the counter electrode and a potassium chloride saturated calomel electrode (SCE) as the reference electrode. Therefore, all the potential values reported in this paper are with reference to SCE, unless mentioned otherwise. All experiments were performed at ambient temperatures 25±2 °C with 10 ml working solution, and the electrochemical solutions were thoroughly deaerated, whenever required, by purging with high-purity nitrogen gas.

Preparation of functionalized graphene

The as-obtained graphene sheets were refluxed with concentrated nitric acid for 6 h. The reaction mixture was diluted with pure water and filtered. The separated functionalized graphene was thoroughly washed with pure water till the filtrate becomes almost neutral. After drying under vacuum at 50 °C, the residue, i.e., functionalized graphene sheets, was used for modifying the surface of graphite electrode.

Preparation of the working electrode

The working electrode is prepared by inserting a graphite rod (diameter of 6 mm) in a teflon tube with an inner diameter of 6 mm, and a copper wire is used for the purpose of electrical contact. The exposed surface of the graphite rod was polished with emery papers of 1,000, 800, 6/0, 4/0, and 2/0 grade till a mirror-like shine on the surface was obtained. Then it was sonicated with doubly distilled water, dried, and modified by

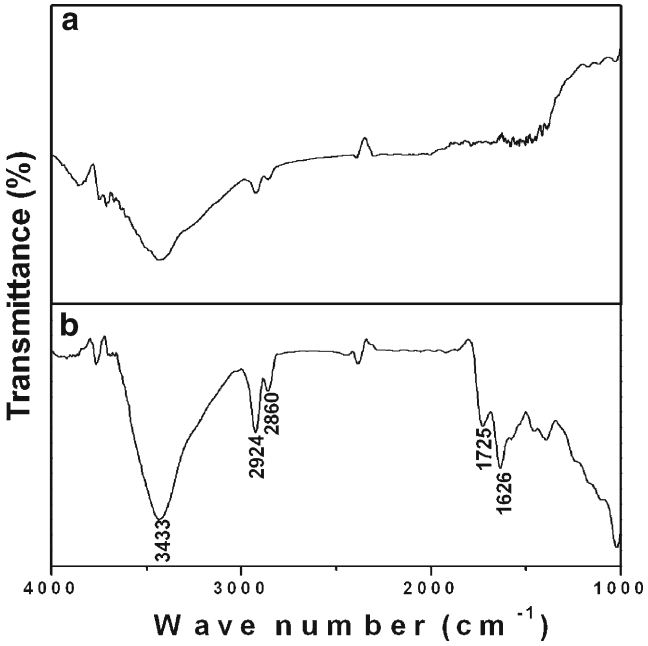

Fig. 1 FT-IR spectra of pristine graphene (**a**) and functionalized graphene (**b**)

gently rubbing against functionalized graphene sheets. The attachment of functionalized graphene on graphite electrode will take place due to the mechanical force as well as action of adsorption [23, 24]. Prior to use as the working electrode, the modified electrode was carefully washed with doubly distilled water to remove the loose graphene sheets. Henceforth, the modified working electrode is designated as "functionalized graphene modified graphite electrode" (FGGE).

Results and discussion

Characterization of FGGE using fourier transform infrared

Fourier transform infrared (FT-IR) spectra were used to characterize the functionalized graphene. FT-IR spectra were recorded on a Shimadzu (Japan) FT-IR spectrometer. FT-IR spectra were taken with a resolution of 4 cm^{-1}. Samples were thoroughly ground with exhaustively dried potassium bromide, and the pellets were prepared by compression under vacuum. The FT-IR spectra of graphene sheets before and after functionalization are presented in Fig. 1 The spectrum of pristine (curve a) graphene shows the only noteworthy band at 3,433 cm^{-1} which is attributed to the O–H stretching vibrations of phenolic groups. On the other hand, the spectrum of functionalized graphene (curve b) shows a strong absorption at 1,626 cm^{-1} which is attributed to the bending vibrations of O–H groups and sp^2 characteristics of graphene sheets. The peak at 1,722 cm^{-1} is attributed to the C=O stretch of the carboxylic group. Bands at 2,924 and 2,857 cm^{-1} represent the stretching of the CH_2 groups. But there was no such a band in the spectrum of pristine graphene. In addition, there is an increase in the intensity of the band due to the phenolic groups, indicating an increase in the number of phenolic groups on the surface of functionalized graphene [25]. These results suggest that the edges of

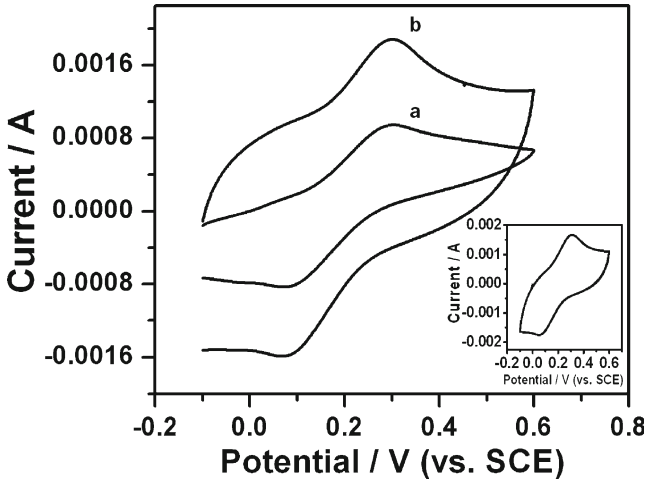

Fig. 3 Cyclic voltammograms of bare graphite (**a**) and FGGE (**b**) electrodes in 1 mM $[Fe(CN)_6]^{4-/3-}$. *Inset*: CV (10 cycles) of FGGE in 1 mM $[Fe(CN)_6]^{4-/3-}$, scan rate at 0.1 Vs^{-1}

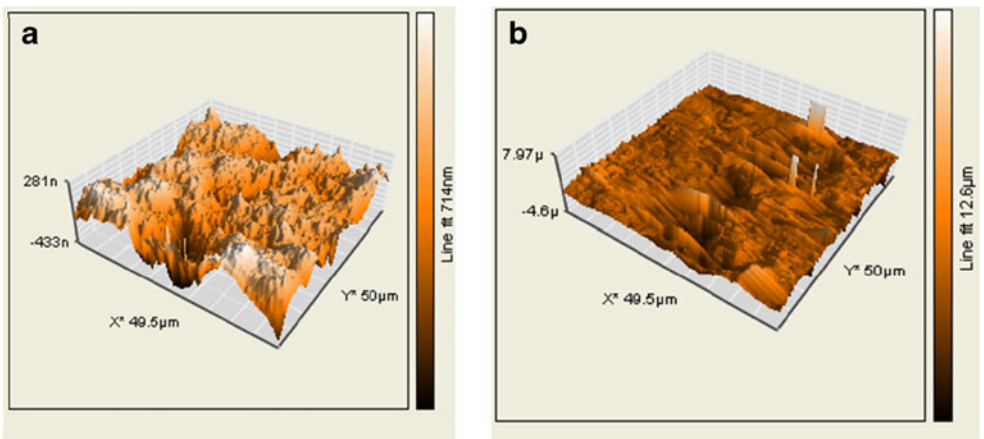

Fig. 2 AFM images of bare graphite electrode (**a**) and FGGE (**b**)

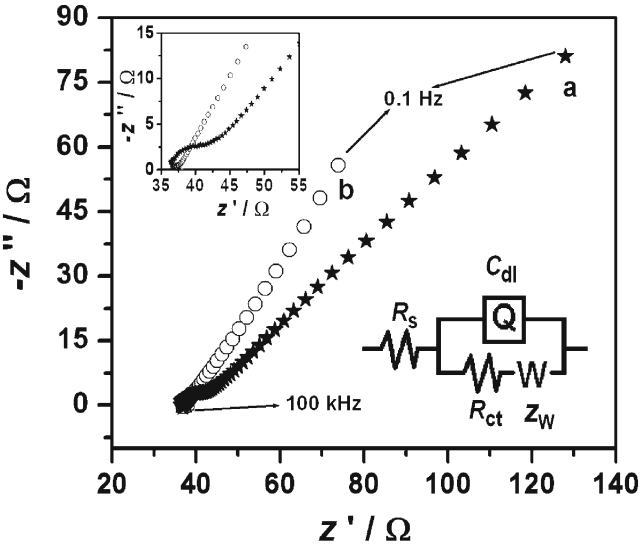

Fig. 4 Nyquist impedance plots of bare graphite (**a**) and FGGE (**b**) electrodes in 1 mM $[Fe(CN)_6]^{4-/3-}$. Frequency ranges from 100 kHz to 100 mHz, amplitude at 5 mV. *Inset* shows equivalent Randles circuit

graphene sheets have been oxidized to carboxylic and phenolic groups upon functionalization. Furthermore, the incorporation of functional groups into graphene leads to structure defects [26, 27], which is confirmed from Raman spectroscopy (figure not shown).

Characterization of FGGE using AFM

In order to confirm the roughness, the interface was viewed by AFM, and the observed images are shown in Fig. 2. AFM observations were made with an atomic force microscope (Nanosurf Easyscan 2) operated in the contact mode using silicon cantilever in ambient air. The surface roughness was calculated as the root mean square (RMS) roughness determined from root mean square analysis over the scan areas of 50 μm×50 μm. The RMS roughness thus found for bare graphite electrode was 197.9 nm. Similarly, for FGGE, the roughness value was found to be 1,072 nm. This large increase in roughness of the surface of FGGE is due to the adsorption of FG nano sheets on the graphite electrode. The functionalized graphene sheets have lateral dimensions from a few hundred nanometers to several micro meters. The average thickness of a single-layer graphene sheet was 50 nm.

Table 1 Kinetic parameters obtained upon fitting the experimental impedance data with the equivalent circuit

Electrode	R_s (Ω)	R_{ct} (Ω)	C_{dl} (mF)	Z_w (Ω)
Bare graphite	36.78	47.78	0.022	0.010
FGGE	37.67	0.009	2.85	0.017

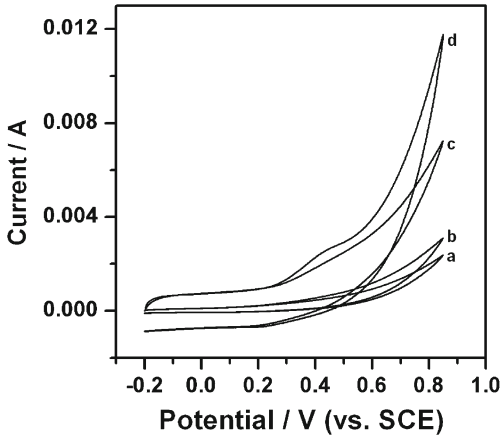

Fig. 5 CV curves of bare graphite electrode and FGGE in the absence (curves *a* and *c*) and presence of 5 mM of glucose (curves *b* and *d*), respectively, in 0.5 M NaOH. Scan rate: 0.1 Vs^{-1}

Characterization of FGGE using cyclic voltammetry

The cyclic voltammetric behavior of graphite electrode before and after its modification with functionalized graphene was studied using 1 mM $[Fe(CN)_6]^{3-/4-}$ as an electrochemical label in 0.1 M PBS (pH 7.0) containing 0.1 M KCl. Figure 3 presents the cyclic voltammograms of bare graphite and modified graphite electrodes. The bare electrode gives a pair of quasi-reversible redox peaks (curve a). After the electrode is modified with functionalized graphene, the peak current of redox waves is increased more than two times without much change in ΔE_p value (curve b). This current enhancement is due to electrocatalytic activity of functionalized graphene.

Characterization of FGGE using electrochemical impedance spectroscopy

Electrochemical impedance spectroscopy (EIS) is an important and powerful tool to study the changes that occur at the

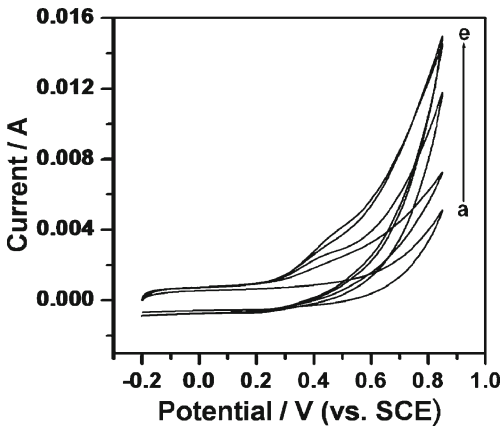

Fig. 6 Cyclic voltammograms of FGGE in the presence of 0, 3, 5, 9, and 12 mM of glucose in 0.5 M NaOH. Scan rate: 0.1 Vs^{-1}

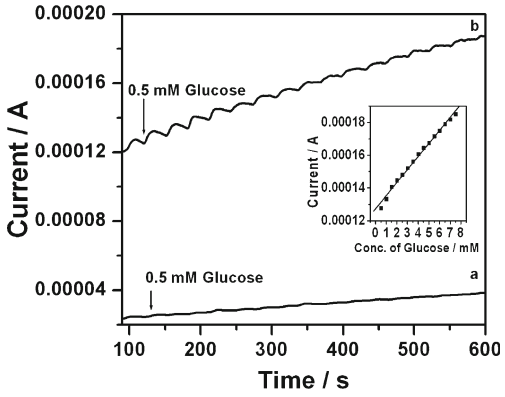

Fig. 7 Chronoamperometric response of bare graphite (curve *a*) and FGGE (curve *b*) upon successive addition of 0.5 mM glucose in 0.5 M NaOH at an applied potential +0.4 V. Calibration curve shown in the *inset*

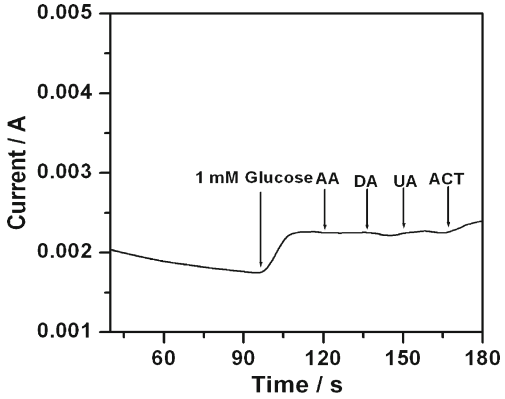

Fig. 8 Chronoamperometric response of FGGE upon subsequent addition of glucose (1 mM), ascorbic acid (250 μM), dopamine (100 μM), uric acid (100 μM), and acetaminophen (100 μM) in 0.5 M NaOH at an applied potential +0.4 V

electrode/electrolyte interface. A typical complex plane impedance spectrum (Nyquist plot) consists of a semicircle domain in the high-frequency region corresponding to electron transfer-controlled process and a linear part at low-frequency region corresponding to diffusion-controlled process. Figure 4 shows the EIS Nyquist plots of bare graphite and FGGE measured in the frequency range from 100 kHz to 100 mHz at the formal potential of $[Fe(CN)_6]^{3-/4-}$ redox couple in 0.1 M PBS (pH 7. 0) containing 0.1 M KCl and 1 mM $[Fe(CN)_6]^{3-/4-}$ which is used as a redox label to probe the electrochemical properties at the charged interface. The Nyquist plot of bare graphite electrode has a small but clear semicircle domain indicating that there is some impedance for movement of electrons at bare electrode surface. On the other hand, the Nyquist plot of FGGE is almost a straight line without any semicircle domain suggesting no hindrance to the electron transfer. This may be attributed to the good conductivity of the surface-deposited functionalized graphene. The spectra were fitted to equivalent Randles circuit which is shown in the inset of Fig. 4. The circuit includes the ohmic resistance of the electrolytic solution (R_s), the Warburg impedance (Z_w) resulting from the ions from electrolytic solution to the electrode, the double layer capacitance (C_{dl}), and the interfacial charge transfer resistance (R_{ct}). The two components R_{ct} and C_{dl} depend on the dielectric and insulating features at the interface. In the Randles circuit model, R_{ct} and Z_w are both in parallel to the C_{dl}. The values of the fitting parameters of the electrode are summarized in Table 1. The R_{ct} value of the functionalized graphene (FG) modified is much smaller than that of the bare graphite electrode, suggesting that the FG was facilitating the easy electron transfer. Further, the C_{dl} value for the modified electrode is much higher than that for the bare electrode, revealing that the ferricyanide ions can easily diffuse through the FG layer. These results are in good agreement with those of cyclic voltammetry (CV) studies.

Electrocatalytic activity of glucose at FGGE

The electrochemical behavior of β, D (+)-glucose at both bare graphite and FGGE was studied in an alkaline solution using cyclic voltammetry. Figure 5 presents the CV behavior of bare

Table 2 Comparison of analytical parameters of different non-enzymatic glucose sensors

Electrode	Applied potential	Linear range	Sensitivity	LOD	Reference
Porous gold	+350 mV	2–10 mM	11.8 μA mM^{-1} cm^{-2}	5 μM	[28]
MWCNTs	+200 mV	2 μM–11 mM	4. 36 μA mM^{-1} cm^{-2}	1 μM	[29]
CuO nanowires	+330 mV	0.4 μM–2 mM	0.49 μA mM^{-1} cm^{-2}	0.049 μM	[30]
Pt nanotubule	+400 mV	2–14 μM	0.1 μA mM^{-1} cm^{-2}	1 μM	[31]
Porous Cu_2O microcubes	–	0–1.5 mM	50.6 μA mM^{-1} cm^{-2}	–	[32]
Nanoporous Pt	–	1–10 mM	1.65 μA mM^{-1} cm^{-2}	–	[33]
Pt–Pb/CNTs	+300 mV	up to 11 mM	17.8 μA mM^{-1} cm^{-2}	1.8 μM	[34]
Mesoporous Pt	+400 mV	0–10 mM	9.6 μA mM^{-1} cm^{-2}	–	[35]
Pd/Graphene	+500 mV	10 μM–5 mM	–	1 μM	[36]
FGGE	+400 mV	0.5–7.5 mM	28.4 μA mM^{-1} cm^{-2}	10 μM	This work

LOD limit of detection

graphite electrode and FGGE in the absence (curves a and c) and presence of 5 mM of glucose (curves b and d), respectively, in 0.5 M NaOH at a scan rate of 100 mV s^{-1} at the potential range from −0.2 to 0.8 V. In the figure, it is evident that both the bare and modified electrodes have responded to the added glucose. However, the current enhancement is very high for the modified electrode compare to that for the bare electrode in the presence of the same amount of glucose (5 mM). This shows the good electrocatalytic activity of FGGE towards glucose.

Further, the effect of change in concentration of glucose on the CV behavior of modified electrode was studied. As shown in Fig. 6, the electrode responded well to different concentrations of glucose.

Amperometric response of FGGE towards glucose

Amperometric response of an electrode is generally studied by measuring the current response at fixed potential by adding the known amount of analyte at regular intervals using chronoamperommetry. Figure 7 depicts the amperograms obtained for the bare graphite (curve a) and FGGE (curve b) obtained by successively adding 0.5 mM of glucose solution in 0.5 M NaOH solution. The optimized potential for the electrochemical oxidation of glucose was determined to be +0.4 V. The modified electrode showed good linear response to the change of glucose concentration in the range from 0.5 to 7.5 mM, producing steady state signal within 8 s. The corresponding linear regression is obtained for the calibration plot is $1.2732\times10^{-4}+7.9744\times10^{-6}$ [glucose] (R=0.9962). From the slope of the calibration plot, the sensitivity of the electrode is determined to be 7.974 μA mM^{-1} or 28.4 μA mM^{-1} cm^{-2}. The limit of detection was found to be 10 μM (S/N=3). In Table 2, the sensivity and other analytical parameters of proposed electrode are compared with those of some of electrodes reported earlier [28–36].

Interference studies at FGGE

In order to apply the proposed sensor to the determination of glucose in real samples, a study of discrimination against the possible interferents was carried out using chronoamperometry. Ascorbic acid and uric acid are the most common and potentially important interferents for a glucose biosensor in a clinical setting because these substances are co-oxidized at similar potentials, producing noise anodic current and also reducing the sensitivity of the biosensor. Figure 8 shows the effect of AA, DA, UA, and ACT on the sensitivity of the biosensor to glucose in a stirred 0.5 M NaOH at an applied potential of +0.4 V. When 1 mM of glucose was injected, there was an immediate increased current. Further injection of AA (250 μM), DA (100 μM), UA (100 μM), and ACT (100 μM) did not cause any interference on the current response. The negligible interference from these substances is due the negative operating potential and the much higher sensitivity of the biosensor towards glucose.

Stability of FGGE

The stability of FGGE was studied by running the CV (10 cycles) in 0.1 M PBS (pH 7.0) containing 0.1 M KCl and 1 mM $[Fe(CN)_6]^{3-/4-}$ at a scan rate of 100 mV s^{-1}. The inset in Fig. 1 shows the results of this study. According to this result, there was no significant change in the redox peak currents or peak potentials. This confirms the strong adsorption of functionalized graphene on the graphite electrode surface and thus confirming the stability of FGGE.

Conclusion

A new non-enzymatic amperometric glucose sensor using functionalized graphene is successfully developed. The linear range of glucose, sensitivity, detection limit response time, selectivity, and stability are found to be excellent. Thus, the application of proposed electrode to real samples appears to be promising.

Acknowledgments The authors gratefully acknowledge the financial support from the Department of Atomic Energy—Board of Research in Nuclear Sciences, Government of India. We thank Sri. A.V.S. Murthy, Honorary secretary, Rashtreeya Sikshana Samiti Trust, Bangalore, and Dr. P. Yashoda, Principal, S.S.M.R.V. Degree College, Bangalore, for their continuous support and encouragement.

References

1. Clark LC Jr, Lyons C (1962) Ann New York Acad Sci 102:29–45
2. Park S, Chung TD, Kim HC (2003) Anal Chem 75:3046–3049
3. Huang J-F (2009) Chem Commun 10:1270–1272
4. Hsiao MW, Adzic RR, Yeager EG (1996) J Electrochem Soc 143:759–767
5. Ernst S, Heitbaum J, Hamann CH (1979) J Electroanal Chem Interfacial Electrochem 100:173–183
6. Huang J-F (2008) Electroanalysis 20:2229–2234
7. Ryu K, Kim C, Park C, Choi B (2004) J Am Chem Soc 126:9180–9181
8. Li L-H, Zhang W-D (2008) Microchim Acta 163:305–311
9. Watanabe T, Einaga Y (2009) Biosens Bioelectron 24:2684–2689
10. Myung Y, Jang DM, Cho YJ, Kim HS, Park J, Kim J, Choi Y, Lee CJ (2009) J Phys Chem C 113:1251–1259
11. Lu L-M, Li H-B, Qu F, Zhang X-B, Shen G-L, Yu R-Q (2011) Biosens Bioelectron 26:3500–3504
12. Pletcher D (1984) J Appl. Electrochem 14:403–415
13. Burke LD (1994) Electrochim Acta 39:1841–1848
14. Stoller MD, Park SJ, Zhu YW, An JH, Ruoff RS (2008) Nano Lett 8:3498–3502
15. Wang X, Zhi LJ, Mullen K (2008) Nono Lett 8:323–327
16. Vivekchand SRC, Rout CS, Subrahmanyam KS, Govindaraj A, Rao CSRJ (2008) J Chem Sci 120:9–13

17. Ao ZM, Yang J, Lee S, Jiang Q (2008) J Chem Phys Lett 46:276–279
18. Ang PK, Chen W, Wee ATS, Loh KP (2008) J Am Chem Soc 130:14392–14393
19. Wang Y, Li YM, Tang LH, Lu J, Li JH (2009) Electrochem Commun 11:889–892
20. Mallesha M, Manjunatha R, Nethravathi C, Suresh GS, Rajamathi M, Melo JS, Venkatesha TV (2011) Bioelectrochemistry 81:104–108
21. Prasanna Kumar S, Manjunatha R, Nethravathi C, Suresh GS, Rajamathi M, Venkatesha TV (2011) Electroanalysis 23:842–849
22. Shan C, Yang H, Song J, Han D, Ivaska A, Niu L (2009) Anal Chem 81:2378–2382
23. Wang Z-H, Liang Q-L, Wang Y-M, Luo G-A (2003) J Electroanal Chem 540:129–134
24. Qiaocui S, Tuzhi P, Yunu Z, Yang CF (2004) Electroanalysis 17:857–861
25. Oh S-D, Choi S-H, Lee B-Y, Gopalan A, Lee KP, Kim S-H (2006) Ind Eng Chem 12:156–160
26. Kou L, He H, Gao C (2010) Nano-micro Lett 2:177–183
27. Geng D, Yang S, Zhang Y, Yang J, Liu J, Li R, Sham T-K, Sun X, Ye S, Knight S (2011) Appl Surf Sci 257:9193–9198
28. Li Y, Song YY, Yang C, Xia XH (2007) Electrochem Commun 9:981–988
29. Ye JS, Wen Y, Zhang WD, Gan LM, Xu GQ, Sheu FS (2004) Electrochem Commun 6:66–70
30. Zhuang ZJ, Su XD, Yuan HY, Sun Q, Xiao D, Choi M (2008) Analyst 131:126–132
31. Yuan JH, Wang K, Xia XH (2005) Adv Funct Mater 15:803–809
32. Zhang L, Li H, Ni Y, Li J, Liao K, Zhao G (2009) Electrochem Commun 11:812–815
33. Joo S, Park S, Chung TD, Kim HC (2007) Anal Sci 23:277–281
34. Cui HF, Ye JS, Zhang WD, Li CM, Luong JHT, Sheu FS (2007) Anal Chim Acta 594:175–181
35. Park S, Chung TD, Kim HC (2003) Anal Chem 75:3046–3049
36. Lu L-M, Li H-B, Qu F, Zhang X-B, Shen G-L, Yu R-Q (2011) Biosens Bioelectron 26:3500–3504